LINKING MICROSTRUCTURE AND HIGH TEMPERATURE DUCTILITY IN ALUMINIUM ALLOYS 6XXX

Lassance D., Schmitz M., Delannay F. and Pardoen T.
Département des sciences des Matériaux, Université catholique de Louvain, IMAP, Belgium.

ABSTRACT

The link between the hot deformation damage behaviour of two aluminium alloys of the 6xxx series and the microstructural evolution occurring during the homogenisation treatment is studied in order to improve the understanding and the control of the damage resistance during extrusion. The hot ductility and deformability of these alloys were investigated from a campaign of uniaxial tension tests by varying the deformation temperature and the second phase particles content. Large β-AlFeSi particles impair hot ductility by nucleating flat voids which grow and coalesce faster than rounded voids. Finite element simulations based on an enhanced version of the Gurson model are used to more quantitatively relate microstructure and ductility. High homogenisation temperatures and long soaking times are shown to improve the transformation of the brittle platelike monoclinic β-AlFeSi particles to the more rounded cubic α-AlFeSi particles, which results in superior hot deformability and ductility. By comparing the calculated evolutions of maximum ductility for the different alloys (and different homogenisation treatments) with the full scale extrusion trials made with the alloy AA6060, theoretical evolutions of the maximum extrusion speed were extrapolated. Our predictions shows a maximum ram speed for the alloy AA6005A which is half of that of the alloy AA6060.

1 INTRODUCTION

For commercial aluminium extrusion alloys, a homogenisation heat treatment of the as-cast material is required to improve ductility and enable efficient extrusion. The optimisation of the extrusion process will depend on a thorough understanding of the homogenisation kinetics and, in particular, of the morphological evolution of the intermetallics particles during the homogenisation. Damage initiation occurs in 6xxx alloys by decohesion or fracture of the intermetallic inclusions as showed by Agarwal *et al.* [1], Bae and Ghosh [2], and Toda and Kobayashi [3]. The resistance to failure directly depends on the second phase particle content. These particles often located along the grain boundaries can be several microns large, and do not contribute to strengthening. The Fe-bearing intermetallic particles such as β-Al_5FeSi and α-$Al_{12}(Fe,Mn)_3Si$ are typical of the 6xxx alloys and have a significant influence on formability. Their morphology and nature vary depending on the chemistry and thermal treatments. The brittle plate-like monoclinic β phase is associated to poor hot workability. This unfavourable effect can be improved by performing a long homogenisation treatment at high temperature, by which the β phase transforms to the more rounded, metastable, cubic α phase.

The link between hot deformation damage behaviour of two aluminium alloys of the 6xxx family (AA6060 and AA6005A) and microstructural evolution during the homogenisation treatment is studied and compared with the behaviour at room temperature. The goal of this work is to improve the understanding and the control of the damage resistance during hot extrusion.

The microstructure evolution (β → α transformation) is studied by energy dispersive X-ray analysis (EDS) coupled with scanning electron microscope (SEM). The accompanying change in morphology is measured using image analysis. The hot ductility is investigated from a campaign of uniaxial tension tests on smooth and notched cylindrical rods at various deformation temperatures with different second phase particles contents. Finite elements (FEM) simulations based on an enhanced micromechanics-based void growth model are used to more quantitatively relate microstructure and ductility.

2 EXPERIMENTAL

The alloys used in the present investigation were cast industrially. Their chemical composition are 0.49 Mg, 0.43 Si, 0.22 Fe, 0.02 Mn for alloy AA6060 and 0.56 Mg, 0.59 Si, 0.18 Fe, 0.04 Mn for alloy AA6005A. Soaking experiments were performed at 585°C and 600°C with a 30'-300' soak. An energy dispersive X-ray analyser (EDS) was used for identification and quantification of the intermetallic phases. Computer based image analysis was used for measuring the particle morphology change.

3 MICROMECHANICAL MODEL FOR VOID GROWTH AND COALESCENCE

The model developed by Pardoen and Hutchinson [5] was used to obtain a theoretical prediction of the maximum ductility before fracture. The model is well suited for the present case as it incorporates void shape effects which is key to capture the impact of the $\beta \rightarrow \alpha$ transformation on the ductility. The void shape is here directly linked with the intermetallic particles aspect ratio when void nucleation occurs by interface decohesion. The voids are considered spheroidal with initial radii R_{z0} (z is the axis of symmetry) and $R_{x0}=R_{y0}$. The void aspect ratio is defined as $W_0 = R_{z0}/R_{r0}$. A description of the model can be found elsewhere [4].

In order to apply the void growth model, the material flow properties must be known as well as three microstructural parameters: (1) *the initial aspect ratio of the voids* W_0, which will depends on the particles shape and on the damage nucleation mode (which varies with deformation temperature); (2) *the initial void distribution index* λ_0, defined as L_z/L_x, where L_z and L_x characterise the particle spacing in the direction of z axis of the void and in the transverse direction respectively; (3) *the initial void volume fraction* f_0, which can be related to the initial inclusions fraction (see further). Void nucleation is assumed to occur at the beginning of straining. An accurate estimate of the true stress-true strain curve at large-deformation was obtained using an inverse methodology based on the FE simulation of the tensile test after necking, matching all measurable quantities (see e.g. Norris *et al.* [5]).

4 EXPERIMENTAL RESULTS

4.1 Microstructure evolution

As-cast samples of aluminium alloys AA6060 and AA6005A were homogenised at 585°C and 600°C for different periods of time. During the heat treatment, several processes take place, such as the transformation of interconnected plate-like monoclinic β-Al_5FeSi particles into more rounded discrete cubic α-$Al_{12}(Fe,Mn)_3Si$ particles. The transformation rate was measured as well as the accompanying particle shape change, which is deemed to be the most important parameter for obtaining a good extrudability. The results are presented in Fig. 2. We can see the marked difference in kinetics of the $\beta \rightarrow \alpha$ transformation at 585°C and at 600°C.

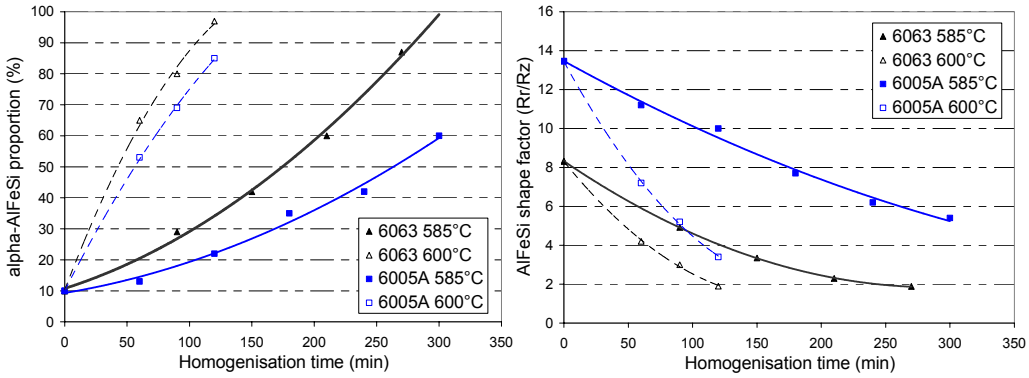

Figure 2: Evolution of the α-$Al_{12}(Fe,Mn)_3Si$ particles proportion (%) and of the mean aspect ratio (*1/W*) with the homogenization time.

4.2 Damage nucleating mechanisms

In situ tensile testing at 20°C and interrupted tensile tests at 550°C were performed in order to investigate the different damage nucleation modes. At room temperature, the particles oriented in the range 0-45° with respect to the loading direction lead to particle fracture, whereas the particles oriented in the range 45-90° lead to particle/matrix interface decohesion (Fig. 3). As the particles are more or less uniformly distributed at grain boundaries, we can consider that 50% of them leads to fracture and 50% to debonding. It seems that at this temperature, all the particles give rise to a void. On the other hand, at high temperature, damage is always initiated by particle/matrix interface decohesion. However, in this case, damage initiation occurs later and only a small fraction of the particles give rise to void nucleation.

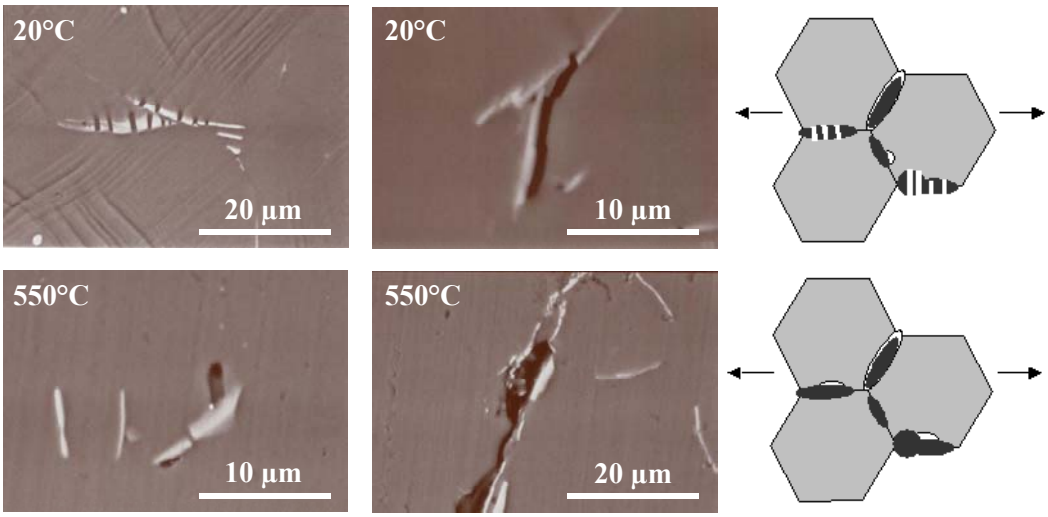

Figure 3: Damage initiation modes observation during in situ and interrupted tensile tests at 20°C (a) and 550°C (b).

5 ELASTO-PLASTIC FE SIMULATION OF THE UNIAXIAL TENSILE TESTS

Tensile tests were simulated by FE calculations using the commercial software Abaqus. A user defined material subroutine implementing the extended Gurson model was used for modelling ductile fracture. Controlled displacement simulations are carried out in order to predict the evolution of *cross-section area at fracture (A_f)*. The AlFeSi particle aspect ratio (W_β) and the deformation temperature were varied. The initial parameters of the microstructure were identified based on the in-situ observations. At 20°C, all the elongated β-AlFeSi particles gives rise to voids (50% of the particles by fracture – 50% by particle/matrix decohesion). The particles which fracture give rise to an average number of voids equal to n = 3.35 (as measured experimentally). These voids are very thin and elongated and we assumed their shape parameter, W_0, to be 0.01 (penny shape). The particles leading to decohesion give rise to voids with the same shape parameter as the particles. In each case, we take account only of the β-AlFeSi particles fraction, f_β, and we varied the initial void distribution parameter, λ_0, to fit the experimental results. We used thus:

$$f_0 = f_{0_{decohesion}} + f_{0_{fracture}} = 0.5 f_\beta + 0.5 f_\beta n \frac{W_0}{W_\beta} \quad \text{and} \quad W_0 = \frac{W_\beta f_{0_{decohesion}}}{f_0} + \frac{0.01 f_{0_{fracture}}}{f_0}$$

Above 550°C, the elongated particles gives rise to a void with the same shape as the particle itself. We varied here also the initial void distribution parameter, λ_0, to fit the experimental results.

Linking the experimental relationship between the particles aspect ratio and the homogenisation conditions with the relationship between the ductility and the particles aspect ratio given by modelling, we obtained a relationship between the maximum ductility at fracture in tension and the homogenisation conditions. These results are shown in Figs 4-5. The grey points correspond to experimental values and the kinetics at 585°C and 600°C are compared for the alloy AA6060.

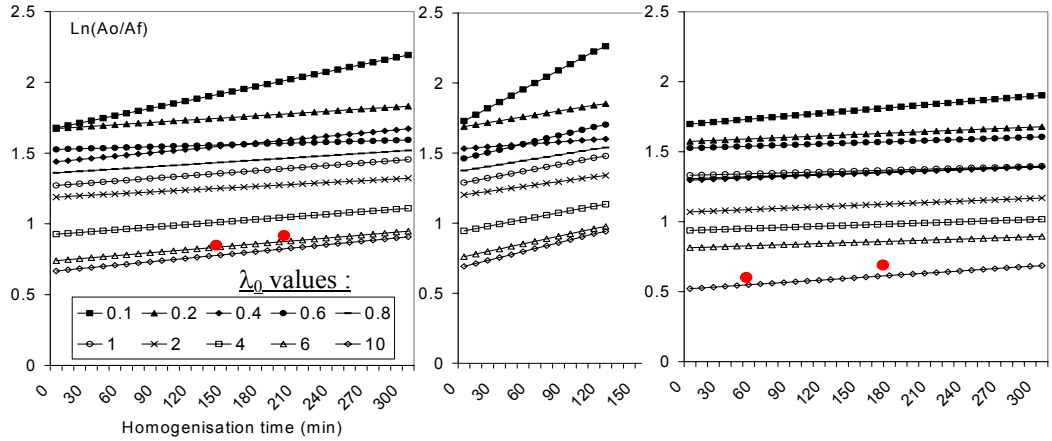

Figure 4: Relationship between the ductility ($\ln(A_0/A_f)$) at 20°C and the homogenisation conditions for the aluminium alloys AA6060 homogenised at 585C (a) and 600°C (b) and for the AA6005A homogenised at 585°C (c) – (•: experimental values).

For the AA6060 as well as for the AA6005A alloys, FEM results correlate to the experiments at room temperature (fracture/debonding mixed mode) for a high value of the parameter λ_0 (~ 6). A large value of λ_0 corresponds to getting the voids closer in the plane of coalescence. It is a way to

introduce heuristically the topology effect related to the accumulation of particles along grain boundaries. It is important to note that once λ_0 is fixed, the evolution of ductility with homogenization time is properly predicted. Further works in this study will consist in validating this on other specimen geometry (notched specimens).

At 590°C, the same conclusion can be drawn from the results concerning the AA6005A alloy. For the AA6060 alloy, the much higher ductility values can only be captured by using unrealistically small λ_0 values. The main reason comes from the fact that the model void nucleation stress was not properly modelled. The AA6060 alloy matrix is so ductile at this temperature that the stress concentration at the matrix/particles interface is very low and thus, only some very large intermetallics play a role in the damage initiation

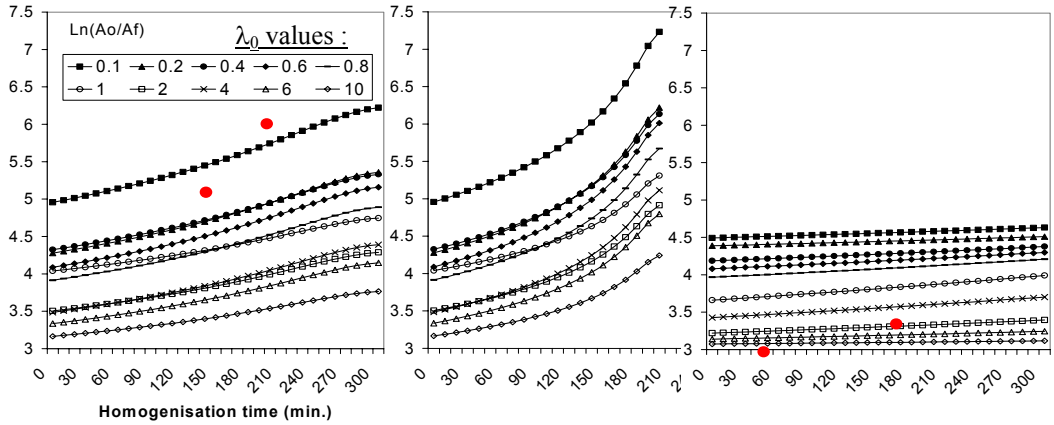

Figure 5: Relationship between the ductility ($\ln(A_0/A_f)$) at 590°C and the homogenization conditions for the aluminium alloys AA6060 homogenised at 585C (a) and 600°C (b) and for the AA6005A homogenised at 585°C (c) – (•: experimental values).

.

6 DISCUSSION AND CONCLUSIONS

During extrusion, the metal temperature increases owing to the deformation and friction in the press. The maximum extrusion speed is usually limited by the hot cracking temperature, which may be associated to the embrittling effect of second phase particles or to the melting caused by eutectic reactions. It usually coincides with the appearance of broken particles on the fracture surface. The present work has firstly demonstrated that the $\beta \rightarrow \alpha$ transformation during the homogenisation heat treatment depends on the chemical composition. In the alloy AA6060 with lower Si and Mg content, the transformation occurs fairly rapidly and depends mainly on homogenisation temperature. However, at a higher Si content (alloy AA6005A), the transformation process is very slow and requires a temperature of 600°C to complete the transformation.

FEM simulations have allowed to relate the maximum ductility (at fracture) with the homogenisation heat treatment parameters. These results give clues about the difference in ductility between the alloys AA6060 and the AA6005A. It gives us also an idea of the saving of time obtained by increasing the homogenisation temperature above 585°C. This temperature is rarely exceeded because of the eutectic melting of the Mg_2Si phase at 585°C, whereas the latter precipitates are dissolved during the very first stage of the homogenisation (during the heating to the homogenisation temperature).

This work aims at predicting the gain in ductility obtained for different alloys with different microstructure for different thermal treatments. Even if the extrudability (i.e. the maximum extrusion speed) cannot be directly linked to the uniaxial tensile section reduction, it gives important information on the possible increase of the ram speed for a determined increase of the homogenisation temperature and/or soaking time. For example, if we relate the increases in extrusion speed (determined in [6] for one simple extruded profile) to the respective increases in homogenisation time, we can see that the evolution in tensile ductility is directly related to the extrudability. By comparing now the calculated evolutions of maximum ductility for the different alloys (and different homogenisation treatments) with the full scale extrusion trials made with the alloy AA6060 [6], we can extrapolate a theoretical evolution of the maximum extrusion speed (considering the same profile). The extrapolated relative maximum extrusion speed (speed divided by a standard speed) are shown in Fig. 6 and compared to the experimental evolution obtained for the alloy AA6060 homogenised at 585°C. The maximum ram speed for the alloy AA6005A is predicted to be half of that of the alloy AA6060. This figure also shows also the theoretical gain that could provide a homogenisation temperature of 600°C.

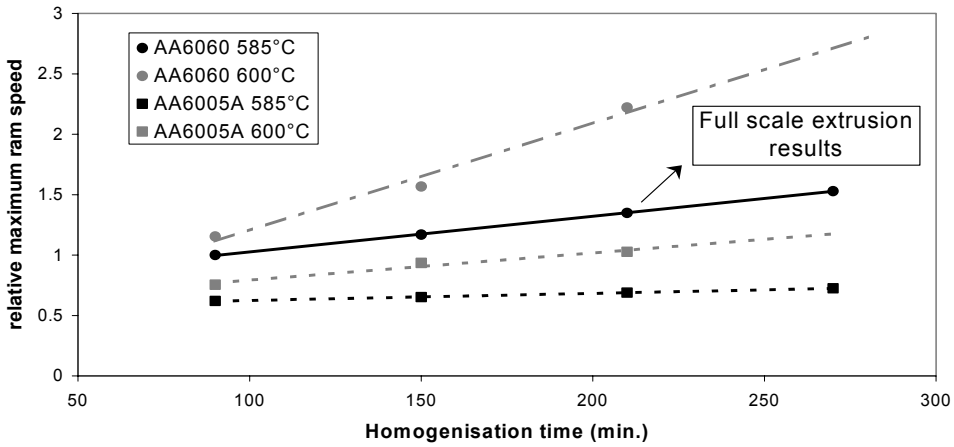

Figure 6: Evolution of the relative maximum extrusion speed with the homogenization time for the alloys AA6060 and AA6005A homogenized at 585°C and 600°C.

ACKNOWLEDGMENTS

The support of the Région Wallonne through a « Subvention Entreprise » (contract # 4436) with Sapa RC profile, Ghlin, Belgium, is gratefully acknowledged. D. Lassance acknowledges also Sapa RC Profile for the supply of material and for the homogenisation heat treatments.

REFERENCES

1. Agarwal, H., Gokhale, A.M., Grahanm, S. and Horstemeyer, M.F., *Met. and Mat. Trans. A*, Vol. 33A, 2599-2606, 2002.
2. Bae, D.H. and Ghosh, A.K., *Acta Materialia*, Vol. 50, 511-523, 2002.
3. Toda, H. and Kobayashi, T., *Mat. Sc. Forum*, Vols 426-432, 393-398, 2003.
4. Pardoen, T. and Hutchinson, J.W., *J. Mech. and Phys. of Sol*., Vol. 48, Issue 12, 2467-2512, 1998.
5. Norris, D.M., Moran, B., Scudder, J.K. and Quinones, D.F., *J. Mech. Phys. Solids*, Vol. 26, 1-19, 1978.
6. Lassance, D., Dille, J., Delplancke, J.L., Pardoen, T., Ryelandt, L. and Delannay, F., *Mat. Sc. Forum*, Vols 426-432, 447-452, 2003.